INSTITUTE OF PHYSICS PUBLISHING NONLINEARITY

Nonlinearity **16** (2003) 1339–1357 PII: S0951-7715(03)53183-8

Spatial pattern formation in a model of vegetation-climate feedback

B Adams and J Carr

Department of Mathematics, Heriot-Watt University, Riccarton, Edinburgh, EH14 4AS, UK

E-mail: b.j.adams@hw.ac.uk

Received 9 September 2002, in final form 1 April 2003
Published 9 May 2003
Online at stacks.iop.org/Non/16/1339

Recommended by J A Glazier

Abstract
We consider a spatial version of Watson and Lovelock's tutorial model of vegetation-climate feedbacks (Watson A J and Lovelock J E 1983 Biological homeostasis of the global environment: the parable of daisyworld *Tellus* B **35** 284–9). Two simple plant types compete on a hypothetical planet, stabilizing the global temperature via an albedo feedback. Numerical solutions show an alternating pattern of the two plant types. A stability analysis shows that there are two mechanisms involved in the pattern formation. A Turing-like process causes the uniform equilibrium state to be unstable to non-constant perturbations and the solution tends towards a striped pattern. This solution is then modified by a mechanism which restricts stripe length and results in subdivision. By calculating the associated temperature function we show how the maximum stripe length can be determined and the stability of different patterns assessed.

Mathematics Subject Classification: 35B40, 35K57, 92D40

1. Introduction

The global climate and terrestrial biosphere form a complex coupled system of which there is an increasingly urgent need to deepen our understanding. Sophisticated climate simulation models can give some insight but their very complexity can often be a hindrance. In contrast to this, very simple, transparent models can be useful for identifying and understanding the fundamental mechanisms of a system. Daisyworld is just such a model. This was originally developed by Watson and Lovelock [1] in support of the idea that the collective biota of the Earth actively manipulates the climate via feedbacks, checks and balances in order to maintain an optimum environment for life to survive. This is not a new concept [2], but was first formulated scientifically in the 1970s by Margulis and Lovelock [3]. Daisyworld aims to demonstrate how such a mechanism could work without the biota having a global knowledge and understanding of the climate system. It is formulated as an ordinary differential equation model describing a hypothetical planet, warmed by a sun and populated by just two types of plant, black daisies and white daisies, identical in every way except colour. The daisies have a temperature dependent growth rate. White surfaces reflect more of the Sun's energy than black and so the variation in local temperature establishes a difference between the two. In the absence of daisies, an increase in solar radiation leads to an equivalent increase in surface temperature. However, Watson and Lovelock [1] found that when the daisies are included in the model their relative areas adjust in such a way that the surface temperature remains very close to the optimum for daisy survival over a broad range of values for the solar radiation.

There has been considerable investigation of the control mechanisms in the daisyworld model [4–6] and a number of extensions including the addition of further trophic levels [7], evolving daisies [8, 9] and two-dimensional space, formulated as a cellular automaton [10]. It has also been investigated as a control system for glucose in the body [11]. A one-dimensional version has been constructed by applying the original equations at each point in space of a one-dimensional projection of a sphere [13]. Numerical solutions of this model resulted in an unexpected striped pattern composed of segregated colonies of black and white daisies. This is interesting as it suggests that there may be a link between the requirement for environmental regulation and the way the vegetation is distributed over the Earth's surface. The purpose of this paper is to provide a relatively detailed mathematical explanation for the patterns observed in that one-dimensional daisyworld model. As well as being an interesting mathematical problem in its own right, this shows that the patterns are a genuine property of the system and not a numerical artefact. It also illuminates the way in which global and local feedback mechanisms can interact. The patterns described in [13] result from a model based on a one-dimensional projection of a sphere. However, in order to understand the mechanisms involved it is expedient to study a similar, but simpler model based one-dimensional projection of a plane. This is given by equations (1)–(3). A more detailed description of the model is given in the appendix.

$$\frac{\partial u}{\partial t} = uf(u, v, w) = u[(1 - \delta(C - 5(u - v - 1) - w)^2)(1 - u - v) - \gamma], \tag{1}$$

$$\frac{\partial v}{\partial t} = vg(u, v, w) = v[(1 - \delta(C - 5(u - v + 1) - w)^2)(1 - u - v) - \gamma], \tag{2}$$

$$\frac{\partial w}{\partial t} = h(u, v, w) + \frac{\partial^2 w}{\partial x^2} = (2 - u + v)R - \sigma w^4 + \frac{\partial^2 w}{\partial x^2} \tag{3}$$

for $-\pi/2 < x < \pi/2$ and with Neumann boundary conditions $w_x = 0$ at $x = \pm\pi/2$.

In equations (1)–(3), $u = u(x, t)$ and $v = v(x, t)$ represent the populations, in terms of the fractional area occupied, of two hypothetical plants (daisies) and $w = w(x, t)$ represents the surface temperature. R, σ, C, δ and γ are constants. $R \sim 200$ determines the incoming solar radiation reaching the surface, $\sigma = 5.67 \times 10^{-8}$ is the Stefan–Boltzmann constant and is used to determine the outgoing long wave radiation at the surface, $C = 295.5$ is the optimal temperature for daisy growth, $\delta = 0.003\,265$ is the intrinsic growth rate and $\gamma = 0.3$ the death rate. These parameter values are retained from the original daisyworld model [1]. The numerical solutions shown in this paper were carried out by applying a 501 point spatial discretization, with a central difference scheme for the derivative, to each partial differential equation. The resultant system of 1503 ordinary differential equations were then solved simultaneously using a variable time-step numerical solver [12]. The objective of this paper is to explain the patterning observed in these numerical solutions. Our analysis requires the value of R to be restricted to a given range and particularly exploits the fact the δ is small. Although the sensitivity of the model to the other parameters values is not considered here, the mathematical analysis should remain valid over a fairly broad parameter space.

2. Overview

The pictures in figure 1, for the large time solutions $u(x)$, $v(x)$, $w(x)$ to equations (1)–(3), are striking. The daisy concentrations are either in a black phase or white phase and at no point in space is there coexistence of the two types. That is, for each x, we have either $u(x) \approx$ constant, $v(x) = 0$ or $u(x) = 0$, $v(x) \approx$ constant. The temperature profile $w(x)$ exhibits mild variations, increasing in the regions where $u(x) = 0$ and decreasing in the regions where $v(x) = 0$. The main objective of this paper is to explain these striped patterns. Here, we present a brief overview.

The initial data for the numerical simulation shown in figure 2 were very close to a uniform black phase equilibrium. In response to a small non-uniform perturbation in w (see the caption of figure 1) the system quickly evolves to a uniform coexistence equilibrium ($u(x) = 0.37$, $v(x) = 0.34$, $w(x) = 298$) by $t = 50$. However, this coexistence equilibrium is unstable via a Turing-like mechanism, the effect of which is clearly seen by $t = 250$. After this, the solution continues to slowly evolve via an additional mechanism to its final, stable, equilibrium state ($t = 1000$). This latter mechanism is the result of the temperature rising in regions in which $u(x) = 0$ (black phase). The larger such a region is, the greater the increase in the local temperature. If this temperature becomes too high it causes an instability in equations (1) and (2) and a small white phase ($v(x) = 0$) subdivides the region. Similarly, a large white phase will reduce the temperature too much and be subdivided by a small black phase.

It turns out to be useful to study the pair of non-spatial ordinary differential equations which result from setting the temperature to be constant in equations (1) and (2). This analysis is carried out in section 3. In section 4, we study the equilibrium solutions of equations (1)–(3) which do not depend on x. De Gregorio *et al* [4] perform a similar analysis but reduce the system to two ordinary differential equations by assuming that the temperature (equation (3))

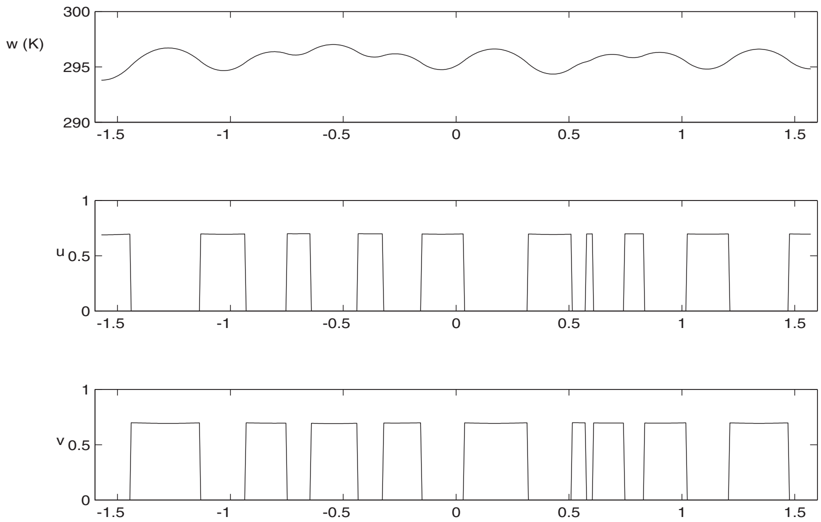

Figure 1. Numerical solution at $t = 1000$ (taken to be equilibrium) of equations (1)–(3) after an aperiodic perturbation to the temperature w. Initial conditions were close to the unstable black phase equilibrium: $u_0 = 0.0001$, $v_0 = 0.377$, $w_0 = 304.98$ everywhere except $w_0(-1.49) = 304.98 + 0.5$, $w_0(-0.38) = 304.98 + 0.2$, $w_0(0.685) = 304.98 - 0.1$. $R = 206.3$. The two daisy populations occupy distinct intervals which do not overlap. Peaks and troughs in the temperature profile match the pattern of the daisies.

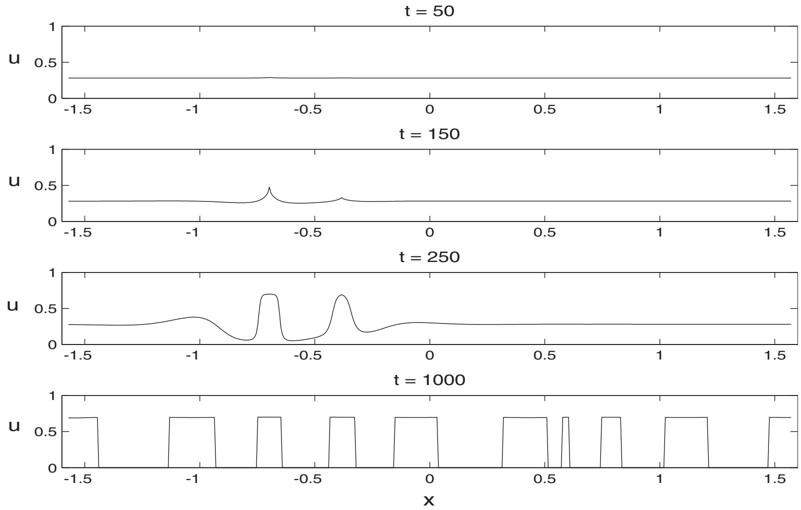

Figure 2. Evolution of the numerical solution for the white daisy population u in equations (1)–(3) after an aperiodic perturbation to the temperature w. Initial conditions were close to the unstable black phase equilibrium: $u_0 = 0.0001$, $v_0 = 0.377$, $w_0 = 304.98$ everywhere except $w_0(-1.49) = 304.98 + 0.5$, $w_0(-0.38) = 304.98 + 0.2$, $w_0(0.685) = 304.98 - 0.1$. $R = 206.3$. At $t = 50$ the system reaches the coexistence equilibrium. By $t = 150$ it is apparent that this is unstable. By $t = 1000$ a stable pattern has been established.

has a much faster timescale and is always at equilibrium. We analyse the full system and in particular show that the coexistence equilibrium is stable to constant perturbations but unstable when diffusion is included. This instability behaves in a similar way to a Turing mechanism to produce a striped pattern, alternating between the all black and all white stable states. This is then further modified by additional instabilities. In order to understand the processes involved in this we study a modified problem, in which there is only one interval of the black phase present, in section 5. We show that there is a maximum possible length, depending on the solar radiation, for a black stripe, and that stripes exceeding this length will subdivide. In section 6 we consider solutions for multi-phase patterns. Finally, we briefly discuss two modifications to equations (1)–(3) and the relevance of the model to the real Earth.

3. Analysis of the ordinary differential equations

To understand the behaviour of the system described by equations (1)–(3) it is helpful to first understand the stability of the system of two ordinary differential equations which arises when w is set to be constant in equations (1) and (2). In particular we find that the all white phase and all black phase equilibria are stable but that the zero and coexistence equilibria are unstable. We also find that the solution develops very slowly in the region close to the coexistence equilibrium. Throughout this section we write $f(u, v)$ for $f(u, v, w)$ and similarly for g. With applications to the full system (1)–(3) in mind we assume that $f(0, 0)$ and $g(0, 0)$ are positive; for the parameter values given this means that w is in the range $286 < w < 305$.

The ordinary differential equations

$$\dot{u} = uf(u, v), \qquad \dot{v} = vg(u, v) \tag{4}$$

have four equilibrium solutions with $0 \leqslant u, v \leqslant 1$: the zero solution $(0, 0)$, the all white phase $(\bar{u}(w), 0)$, the all black phases $(0, \bar{v}(w))$, and the coexistence phase $(\bar{u}_c(w), \bar{v}_c(w))$. To assess their stability we consider the eigenvalues of the linearization of (4) about each of these equilibria.

3.1. Stability of zero equilibrium

The zero solution is unstable, with the linearization having the two positive eigenvalues $f(0,0)$ and $g(0,0)$.

3.2. Stability of all white equilibrium

For the equilibrium $(\bar{u}(w),0)$, $u=\bar{u}$ is a solution of the cubic equation $f(u,0)=0$. Since the coefficient of u^3 in $f(u,0)$ is positive and $f(0,0)>0$, $f(1,0)<0$, there is a unique solution $u=\bar{u}(w)$ with $f_u(\bar{u}(w),0)<0$. We can obtain an approximation to $u=\bar{u}(w)$ by making use of the small parameter δ. Writing the equation $f(u,0)=0$ as $\delta(w-C-5+5u)^2=(1-\gamma-u)(1-u)^{-1}$, we have that

$$\bar{u}(w)=1-\gamma-\gamma\delta(w-C-5\gamma)^2+\mathrm{O}(\delta^2), \tag{5}$$

which is valid if $(w-C-5\gamma)^2$ is not too large. We will make use of this approximation in the study of the stable equilibria of the full set of equations. The eigenvalues of the linearization about $(\bar{u}(w),0)$ are $\bar{u}(w)f_u(\bar{u}(w),0)<0$ and $\lambda(w)=g(\bar{u}(w),0)$. Since $f(\bar{u}(w),0)=0$,

$$\lambda(w)=f(\bar{u}(w),0)+\delta(1-\bar{u}(w))[(C-w-5\bar{u}(w)+5)^2-(w-C-5\bar{u}(w)-5)^2],$$

which simplifies to

$$\lambda(w)=20\delta(1-\bar{u}(w))(C-w-5\bar{u}(w)).$$

The sign of $\lambda(w)$ determines the stability of $(\bar{u}(w),0)$. Using (5), there exists w_1 such that $\lambda(w)>0$ for $w<w_1$ and $\lambda(w)<0$ for $w>w_1$ with $w_1=C-5(1-\gamma)+\mathrm{O}(\delta)$. We can find an exact expression for w_1 by using $f(\bar{u}(w),0)=g(\bar{u}(w),0)=0$ at $w=w_1$. Using $5\bar{u}(w_1)=C-w_1$ in the equation $f(u,0)=0$ we obtain

$$\bar{u}(w_1)=b, \qquad w_1=C-5b, \tag{6}$$

where

$$b=1-\gamma(1-25\delta)^{-1}. \tag{7}$$

Hence, this equilibrium is stable for $w>w_1$ and unstable for $w<w_1$.

3.3. Stability of all black equilibrium

Similarly, there is a unique equilibrium $(0,\bar{v}(w))$ where $v=\bar{v}(w)$ is the solution of $g(0,v)=0$. We can find an approximation to this solution in the same way as above to obtain

$$\bar{v}(w)=1-\gamma-\gamma\delta(w-C+5\gamma)^2+\mathrm{O}(\delta^2), \tag{8}$$

which is valid if $(w-C+5\gamma)^2$ is not too large. The eigenvalues of the linearization about this equilibrium are $\bar{v}(w)g_v(0,\bar{v}(w))$ which is negative and $f(0,\bar{v}(w))=20\delta(1-\bar{v}(w))(w-C-5\bar{v}(w))$. As above, we can find where this eigenvalue is zero by solving the simultaneous equations $f(0,v)=g(0,v)=0$. A calculation shows that $f(0,\bar{v}(w))=0$ when $w=w_2$ with

$$\bar{v}(w_2)=b, \qquad w_2=C+5b. \tag{9}$$

Hence, this equilibrium is stable if $w<w_2$ and unstable if $w>w_2$.

3.4. Stability of coexistence equilibrium

The coexistence phase $(\bar{u}_c(w), \bar{v}_c(w))$ is found by solving $f(u, v) = g(u, v) = 0$. Using the variables $u + v$ and $u - v$, these equations can be solved exactly to obtain

$$\bar{u}_c(w) = \frac{C - w + 5b}{10}, \qquad \bar{v}_c(w) = \frac{w - C + 5b}{10}. \tag{10}$$

Using the formulae for w_1 and w_2 given in (6) and (9) we can also write this as

$$\bar{u}_c(w) = \frac{w_2 - w}{10}, \qquad \bar{v}_c(w) = \frac{w - w_1}{10}. \tag{11}$$

The above shows that the coexistence phase degenerates into the white phase $(\bar{u}(w), 0)$ at $w = w_1$ and into the black phase $(0, \bar{v}(w))$ at $w = w_2$. For $w_1 < w < w_2$, we have that $\bar{u}_c(w)$ and $\bar{v}_c(w)$ lie between 0 and 1 while for w outside this range, either $\bar{u}_c(w)$ or $\bar{v}_c(w)$ is negative. The eigenvalues of the linearization about the coexistence phase satisfy

$$\lambda^2 - \lambda(\bar{u}_c f_u + \bar{v}_c g_v) + \bar{u}_c\bar{v}_c(f_u g_v - g_u f_v) = 0. \tag{12}$$

This equation can be solved exactly to show that there is one negative eigenvalue and a small positive eigenvalue of order δ. We exploit the small parameter δ to prove this instability result; similar calculations will be used in the next section when studying the stability of the coexistence phase for the full equations. Since $w_1 < w < w_2$, all the partial derivatives of f and g are equal to $-1 + \mathrm{O}(\delta)$. Hence, $f_u g_v - g_u f_v = \alpha\delta + \mathrm{O}(\delta^2)$ where α is a constant and using equation (10), $\bar{u}_c f_u + \bar{v}_c g_v = -b + \mathrm{O}(\delta)$. It follows that the equation for the eigenvalues takes the form

$$\lambda^2 + \lambda(b + \mathrm{O}(\delta)) + \bar{u}_c\bar{v}_c\alpha\delta + \mathrm{O}(\delta^2) = 0. \tag{13}$$

Since δ is small, the eigenvalues are $\lambda_1 = -b + \mathrm{O}(\delta) < 0$ and $\lambda_2 = -\alpha b^{-1}\bar{u}_c\bar{v}_c\delta + \mathrm{O}(\delta^2)$. Since $\bar{u}_c\bar{v}_c$ is positive, the sign of λ_2 depends on the sign of α. A straightforward calculation shows that $\alpha = -200(1 - b) < 0$ so that λ_2 is positive and the coexistence phase is unstable.

3.5. Phase plane analysis

Figure 3 shows the phase plane portrait for the ordinary differential equation system (4) for a particular w such that $w_1 < w < w_2$. The stable manifold of the coexistence phase divides the phase plane into regions in which solutions converge either to $(\bar{u}(w), 0)$ or to $(0, \bar{v}(w))$. The unstable manifold $\mathcal{U}$ of the coexistence phase connects to $(\bar{u}(w), 0)$ and $(0, \bar{v}(w))$. A typical solution spends a lot of time near $\mathcal{U}$ before converging to an equilibrium point. To see this, let $y = u + v + \gamma - 1$ and $z = u(u + v)^{-1}$. A calculation shows that

$$\dot{y} = -y(y + 1 - \gamma) + \mathrm{O}(\delta), \qquad \dot{z} = \mathrm{O}(\delta). \tag{14}$$

From (14), y converges to $\mathcal{U}$, which in these coordinates is given by $y = \mathrm{O}(\delta)$, in order one time. The z variable describes the slow flow on $\mathcal{U}$.

4. Space independent equilibria

We now return to the full system, as given by equations (1)–(3) and analyse the stability of solutions which do not depend on x. If (u, v, w) is such a solution then (u, v) is one of the four equilibrium solutions for the ordinary differential equations (4) considered in the previous section and w is a solution of

$$[2 - u(w) + v(w)]R - \sigma w^4 = 0. \tag{15}$$

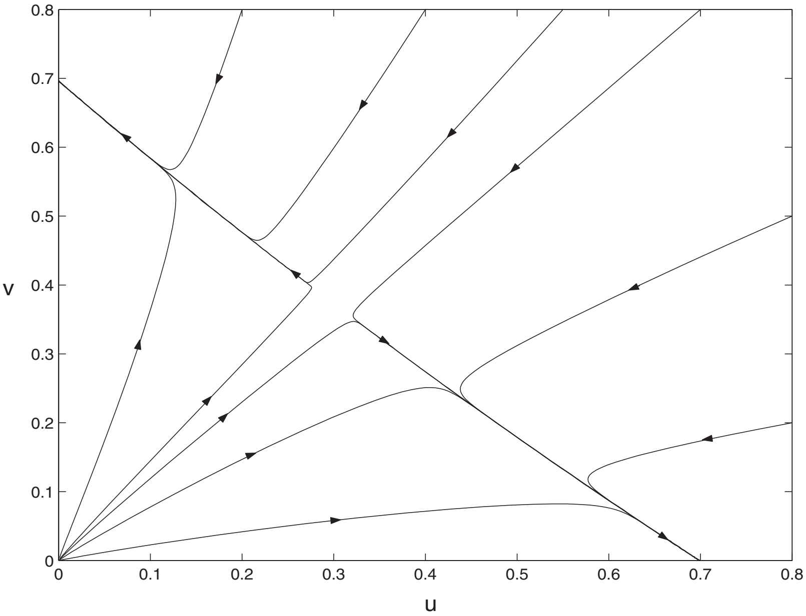

Figure 3. Phase plane for the ordinary differential equation system (4) with constant $w = 296$. The stable manifold of the coexistence phase divides the plane into regions in which solutions converge to either the white only equilibrium or the black only equilibrium.

From the previous section the white phase $(\bar{u}(w), 0)$ is an unstable equilibrium of equation (4) if $w < w_1$. Solving equation (15) with $u = \bar{u}(w)$ and $v = 0$ gives the equilibrium temperature $w = \bar{w}_u$ (note that this assumes $u = \bar{u}(w)$ exists, see remark 1). For the range of values of R that we consider, $\bar{w}_u$ is smaller than w_1. Using this we show that the equilibrium $(\bar{u}(\bar{w}_u), 0, \bar{w}_u)$ of equations (1)–(3) is unstable to constant perturbations. Similarly, we show that the equilibrium solutions of equations (1)–(3) corresponding to the black phase and the zero solution are unstable to constant perturbations. The coexistence phase $(\bar{u}_c(w), \bar{v}_c(w))$ is unstable for the ordinary differential equations (4). We show that the equilibrium solution of equations (1)–(3) corresponding to this is stable to constant perturbations but unstable when diffusion is included.

We assume throughout this section that $\bar{w}_u < w_1$ and that $\bar{w}_v > w_2$. To determine the restrictions that this places on R, consider the equation $[2 + \bar{v}(w)]R - \sigma w^4 = 0$ which has the solution $w = \bar{w}_v$. Since the left-hand side of this equation is a decreasing function of w, $\bar{w}_v > w_2$ implies that $[2 + \bar{v}(w_2)]R > \sigma w_2^4$. Using the formula for w_2 and $\bar{v}(w_2)$ given by (9), we obtain

$$R > \sigma(2+b)^{-1}(C+5b)^4. \tag{16}$$

Similarly, by considering the equation satisfied by $\bar{w}_u$, we obtain $(2 - \bar{u}(w_1))R < \sigma w_1^4$ and

$$R < \sigma(2-b)^{-1}(C-5b)^4. \tag{17}$$

4.1. Stability of zero equilibrium

For constant perturbations to the equilibrium $(0, 0, \bar{w})$, the linearization has one negative eigenvalue h_w and two positive eigenvalues $f(0, 0, \bar{w})$ and $g(0, 0, \bar{w})$. Hence, it is unstable.

4.2. Stability of all white/all black equilibrium

For constant perturbations to the equilibrium $(\bar{u}, 0, \bar{w}_u)$, the linearized matrix is given by

$$A = \begin{bmatrix} \bar{u} f_u & \bar{u} f_v & \bar{u} f_w \\ 0 & g & 0 \\ h_u & h_v & h_w \end{bmatrix}. \tag{18}$$

Let $E(\lambda) = \det(A - \lambda I)$. Then $E(\lambda)$ is a cubic in λ, with leading term $-\lambda^3$, so to prove that A has a positive eigenvalue it is sufficient to show that $E(0) = \det(A) > 0$. Now

$$\det(A) = \bar{u} g [f_u h_w - f_w h_u],$$

where all the functions are evaluated at $(\bar{u}, 0, \bar{w}_u)$. Clearly, h_w and h_u are negative and, since $\bar{w}_u < w_1$, we have that $g(\bar{u}, 0, \bar{w}_u)$ is positive. From the previous section, $f_u < 0$ at the equilibrium. It remains to show that $f_w = 2\delta(C + 5 - \bar{w}_u - 5\bar{u})(1 - \bar{u}) > 0$. Since $\bar{w}_u < w_1 = C - 5b$,

$$f_w > 2\delta(C + 5 - w_1 - 5\bar{u})(1 - \bar{u}) = 10\delta(b + 1 - \bar{u}) > 0,$$

so that $\det(A) > 0$ as required. Hence, the white phase equilibrium is unstable. A similar proof shows that the black phase equilibrium is unstable to constant perturbations.

4.3. Uniqueness and stability of coexistence equilibrium

Before considering the stability of the coexistence phase we show that it is unique. The coexistence phase $(\bar{u}_c(w), \bar{v}_c(w))$ exists for $w_1 < w < w_2$. The corresponding equilibrium temperature $\bar{w}_c$ is a solution of

$$[2 - \bar{u}_c(w) + \bar{v}_c(w)]R - \sigma w^4 = 0.$$

Using equation (10) for $\bar{u}_c(w)$ and $\bar{v}_c(w)$, this can be written as

$$m(w) = \left[2 + \frac{w - C}{5}\right] R - \sigma w^4 = 0. \tag{19}$$

As demonstrated by other researchers [1,6], this shows that the equilibrium temperature in the coexistence phase of the space-independent system does not depend on the values of u or v.

Now $m(w_1) = (2 - b)R - \sigma w_1^4$ and $m(w_2) = (2 + b)R - \sigma w_2^4$. Using the bounds on R given by (16) and (17), $m(w_1) < 0$ and $m(w_2) > 0$. For $w_1 < w < w_2$, $5m'(w) = R - 20\sigma w^3$ so using (16),

$$5(2 + b)m'(w) > \sigma w_2^3 (C - 40 - 15b) > 0.$$

Thus, there exists a unique solution of $m(w) = 0$ and a unique coexistence phase.

We now assess the stability of the coexistence equilibrium. For constant perturbations of the coexistence phase, the eigenvalues of the linearization are the solutions of $E(\lambda) = 0$ where

$$E(\lambda) = \begin{vmatrix} \bar{u}_c f_u - \lambda & \bar{u}_c f_v & \bar{u}_c f_w \\ \bar{v}_c g_u & \bar{v}_c g_v - \lambda & \bar{v}_c g_w \\ h_u & h_v & h_w - \lambda \end{vmatrix}. \tag{20}$$

We make use of the small parameter δ to locate the zeros of $E(\lambda)$. Expanding the third column gives

$$E(\lambda) = (h_w - \lambda) \begin{vmatrix} \bar{u}_c f_u - \lambda & \bar{u}_c f_v \\ \bar{v}_c g_u & \bar{v}_c g_v - \lambda \end{vmatrix} - \bar{v}_c g_w \begin{vmatrix} \bar{u}_c f_u - \lambda & \bar{u}_c f_v \\ h_u & h_v \end{vmatrix} + \bar{u}_c f_w \begin{vmatrix} \bar{v}_c g_u & \bar{v}_c g_v - \lambda \\ h_u & h_v \end{vmatrix}. \tag{21}$$

The first determinant in (21) was calculated in the previous section (see equations (12) and (13)). Hence, the first term in (21) is

$$(h_w - \lambda)[\lambda^2 + \lambda(b + \mathrm{O}(\delta)) + \bar{u}_c\bar{v}_c\alpha\delta + \mathrm{O}(\delta^2)], \tag{22}$$

where $\alpha = -200(1-b) < 0$. A calculation shows that the second and third terms in (21) are of order δ and that the equation $E(\lambda) = 0$ takes the form

$$(h_w - \lambda)[\lambda^2 + \lambda(b + \mathrm{O}(\delta)) + \bar{u}_c\bar{v}_c\alpha\delta + \mathrm{O}(\delta^2)] - 40R(1-b)\bar{u}_c\bar{v}_c\delta + a(\delta)\lambda + \mathrm{O}(\delta^2) = 0, \tag{23}$$

where $a(\delta) = \mathrm{O}(\delta)$. Since δ is small, the eigenvalues are $\lambda_1 = h_w + \mathrm{O}(\delta) < 0$, $\lambda_2 = -b + \mathrm{O}(\delta) < 0$ and $\lambda_3 = \beta\delta + \mathrm{O}(\delta^2)$, where

$$bh_w\beta = 40R(1-b)\bar{u}_c\bar{v}_c - \alpha h_w\bar{u}_c\bar{v}_c. \tag{24}$$

Using $\alpha = -200(1-b)$ and $h_w < 0$, β has the same sign as $-m'(w_c)$ where $m(w)$ is defined by equation (19). We showed above that $m'(w) > 0$ for $w_1 < w < w_2$ so that β is negative. Hence, the third eigenvalue is negative and the coexistence phase is stable to constant perturbations.

4.4. Stability under non-constant perturbations

We now consider perturbations of the form $\cos(kx)$ in the w variable of the coexistence phase. The eigenvalues of the linearization are the solutions of $E(\lambda, k) = 0$ where $E(\lambda, k)$ is the same as that given in (20) except that the term $h_w - \lambda$ is replaced by $h_w - \lambda - k^2$. Hence the equation $E(\lambda, k) = 0$ is the same as (23) except that the term $h_w - \lambda$ is replaced by $h_w - \lambda - k^2$. The eigenvalues are $\lambda_1(k) = h_w - k^2 + \mathrm{O}(\delta) < 0$, $\lambda_2(k) = -b - k^2 + \mathrm{O}(\delta) < 0$ and $\lambda_3(k) = \beta(k)\delta + \mathrm{O}(\delta^2)$, where

$$b(h_w - k^2)\beta(k) = 40R(1-b)\bar{u}_c\bar{v}_c - \alpha(h_w - k^2)\bar{u}_c\bar{v}_c. \tag{25}$$

As above, a calculation shows that $\beta(k)$ has the same sign as $k^2 - m'(w_c)$. Hence the coexistence phase is unstable to a $\cos(kx)$ perturbation for $k^2 > m'(w_c)$. For the parameter values given, the first unstable mode is $k = 6$.

Remark 1. In order to discuss the equilibrium temperatures $\bar{w}_u$ and $\bar{w}_v$ we need $\bar{u}(w)$ and $\bar{v}(w)$ to exist. From the previous section, we need $f(0, 0)$ and $g(0, 0)$ to be positive. A calculation shows that this requires $C + 5 - (1-\gamma)\delta^{-1/2} < w < C - 5 + (1-\gamma)\delta^{-1/2}$. This in turn leads to upper and lower bounds for R.

5. Localization

The results of the previous section show that all the space independent equilibrium solutions for the full system (equations (1)–(3)) are unstable. However, in section 3, it was shown that the black phase and white phase solutions are stable for the non-spatial ordinary differential equations (4). Motivated by this and the numerical results we look for equilibrium solutions of the full set of equations in which we have alternating regions of black and white phases. From the equilibrium solution for equation (3) it is clear that if $u = 0$ (black phase) then w will increase while if $v = 0$ (white phase) then w will decrease. The effect of diffusion means that peaks in the temperature profile will occur over regions in the black phase and troughs will occur over regions in the white phase. Increasing the length of the region in the black phase will result in a higher maximum temperature. If this maximum exceeds the critical stability point $w = w_2$ then, from section 4, the black phase solution will be unstable. Therefore, black regions above a certain length are unstable and will not occur in a stable equilibrium solution. Similarly, large regions in the white phase will not occur in a stable equilibrium since this would result in a minimum temperature below $w = w_1$.

In order to get a more detailed picture of how this mechanism works we now study a problem in which there is only one interval of the black phase present. Throughout this section we study equations (1)–(3) but restrict the daisies to an interval of width M by assuming that (1) and (2) hold for $|x| \leqslant M$ and that $u(x,t) = v(x,t) = 0$ for $|x| > M$.

5.1. Numerical results

Numerically determined equilibrium solutions for the modified system described above are shown in figure 4. When M is small, the black phase occupies the region $|x| \leqslant M$ while the temperature connects the colder region $|x| > M$ to the hottest point at $x = 0$ (figure 4(*a*)). If we increase M this equilibrium becomes unstable and a patch of white phase appears as shown in figure 4(*b*). The timescale of the evolution of the white phase is slow. As shown in figure 5 there is almost no sign of it until $t = 800$ but it then establishes quite rapidly.

5.2. Phase plane and stability analysis

To understand these numerical results we study the equilibrium solution of equation (3) with $u(x) = 0$ for all x , $v(x) = \bar{v}(w(x))$ for $|x| \leqslant M$ and $v(x) = 0$ otherwise. Let

$$k_1(w) = 2R - \sigma w^4, \qquad k_2(w) = R(2 + \bar{v}(w)) - \sigma w^4. \tag{26}$$

Then, by symmetry we need only study:

$$w''(x) + k(w) = 0, \qquad w'\left(-\frac{\pi}{2}\right) = w'(0) = 0 \tag{27}$$

with w, w' continuous at $x = -M$ and where $k(w) = k_1(w)$ for $x < -M$ and $k(w) = k_2(w)$ for $-M < x \leqslant 0$.

The equation

$$w''(x) + k_1(w) = 0 \tag{28}$$

has a saddle point at $w = \bar{w} = (2R\sigma^{-1})^{1/4}$. Since we are looking for a stable equilibrium we assume throughout this section that $\bar{w} < w_2$. For $w > \bar{w}$, k_1, k_1' and k_1'' are negative. Solutions of (28) with $w' = 0$ when $w = \alpha$ are given by

$$w'^2 = 2[K_1(\alpha) - K_1(w)], \tag{29}$$

where $K_1'(w) = k_1(w)$. A schematic phase plane for (28) in the region $w > \bar{w}$ is shown in figure 6(*a*).

The equation

$$w''(x) + k_2(w) = 0 \tag{30}$$

has a saddle point at $w = \bar{w}_v$, and for $w < \bar{w}_v$ we have that k_2 is positive while k_2' and k_2'' are negative. Solutions of (30) with $w' = 0$ when $w = \beta$ are given by

$$w'^2 = 2[K_2(\beta) - K_2(w)], \tag{31}$$

where $K_2'(w) = k_2(w)$. A schematic phase plane for (30) in the region $w < \bar{w}_v$ is shown in figure 6(*b*).

We construct a solution to the boundary value problem (27) by following an orbit of (28) and then switching to an orbit of (30) as shown in figure 6(*c*). To get some insight suppose that w is a solution of (27) with M small. The solution of (28) has to connect $w'(-\pi/2) = 0$

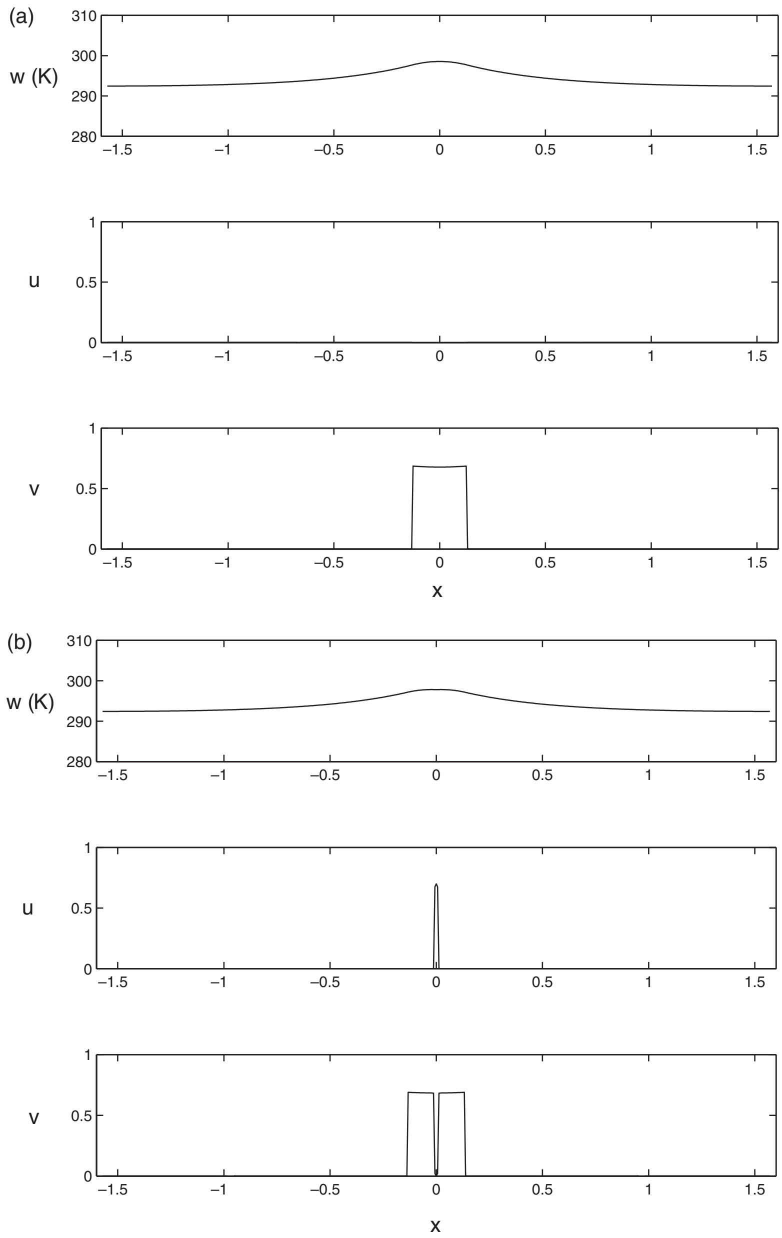

Figure 4. Numerical solutions at $t = 1000$ (taken to be equilibrium) of equations (1)–(3) when $u(x,t) = v(x,t) = 0$ for $|x| > M$. Initially $u(x) = v(x) = 0$ for $|x| > M$ and $u(x) = v(x) = 0.001$ for $|x| \leqslant M$, $w = 292$ for all x. $R = 206.3$. (*a*) $M = 0.132$, (*b*) $M = 0.138$. The presence of a black stripe leads to a peaked temperature profile (*a*). If the width of the stripe exceeds a critical value the maximum temperature exceeds the stability threshold of the black phase equilibrium and the stripe is split by a region of white phase (*b*).

to $w'(-M)$, while the solution of (30) connects $w'(-M)$ to $w'(0) = 0$. If $\alpha = w(-\pi/2)$ is not close to the equilibrium of (28) then $w'(-M)$ will be bounded away from 0. Since M is small it will be impossible for a solution of (30) to connect $w'(-M)$ to $w'(0) = 0$. On the other hand, if $\alpha = w(-\pi/2)$ is close to the equilibrium of (28), then $w(-M)$ will be close to

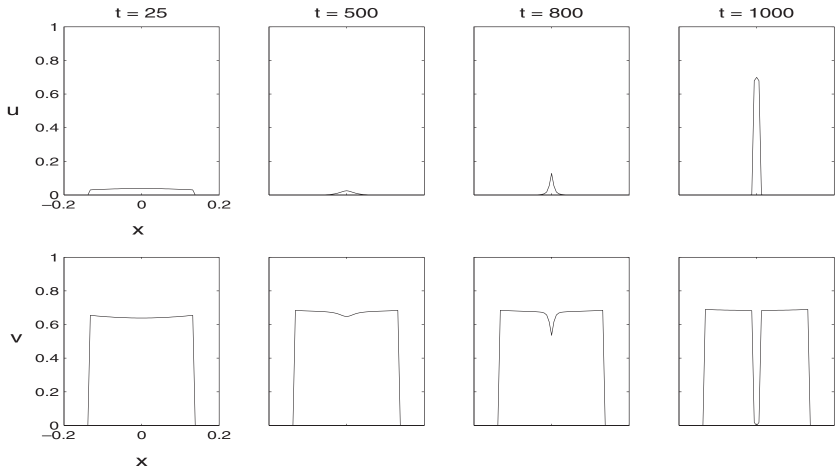

Figure 5. Evolution of a subdividing white phase when equations (1)–(3), with $u(x,t) = v(x,t) = 0$ for $|x| > M$, are solved numerically for $M = 0.138$. Initially, $u(x) = v(x) = 0$ for $|x| > M$ and $u(x) = v(x) = 0.001$ for $|x| \leqslant M$, $w = 292$ for all x. Initially, the transition is slow and little change can be discerned until $t = 800$. After this point the transition becomes quite rapid.

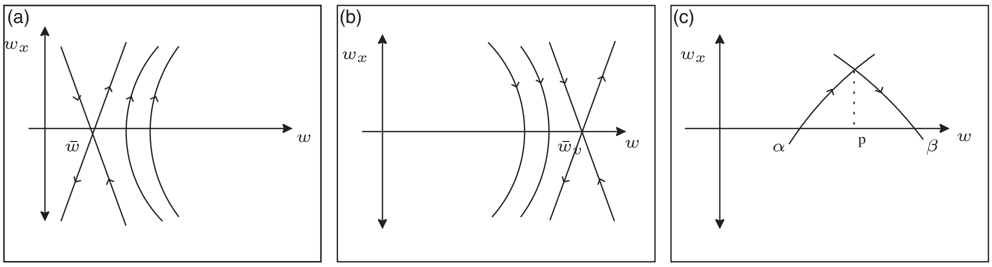

Figure 6. Schematic phase planes of (*a*) equation (28), (*b*) equation (30) and (*c*) the combination of these to find the solution to equation (27).

α and $w'(-M)$ will be small enabling a connection to be made by (30). As M is increased we have to increase $\alpha = w(-\pi/2)$ to get a solution of (27).

5.3. Existence of solutions

Suppose that $w(-\pi/2) = \alpha$, $w(0) = \beta$, and that the orbits of (29) and (31) intersect at $w = p$. Putting $x = -M$ in (29) and (31) we obtain

$$w'^2(-M) = 2[K_1(\alpha) - K_1(p)] = 2[K_2(\beta) - K_2(p)] \tag{32}$$

and we can use this to express $\beta = \beta(\alpha)$ as a function of α. Using (29) and (31), for w to be a solution of (27) with $w(-\pi/2) = \alpha$ we require $L_1(\alpha) + L_2(\alpha) = \pi/2$, where

$$L_1(\alpha) = \int_\alpha^p [2(K_1(\alpha) - K_1(w))]^{-1/2}\,\mathrm{d}w, \tag{33}$$

$$L_2(\alpha) = \int_p^{\beta(\alpha)} [2(K_2(\beta(\alpha)) - K_2(w))]^{-1/2}\,\mathrm{d}w. \tag{34}$$

We outline a proof of the existence of a solution to equation (27). Fix $p > \bar{w}$ and for $\alpha < p$ set $L(\alpha) = L_1(\alpha) + L_2(\alpha)$. We need to show that $L(\bar{\alpha}) = \pi/2$ for some $\bar{\alpha}$. A calculation (see remark 2) shows that $L_1'(\alpha)$ and $L_2'(\alpha)$ are negative. Also, $L(p) = 0$ and $L(\alpha) \to \infty$ either as $\alpha \to \bar{w}$ or for some larger α if the orbit of equation (28) intersects the stable manifold of the equilibrium $\bar{w}_v$ of (30). Hence, $L(\bar{\alpha}) = \pi/2$ for some $\bar{\alpha}$ and we have a solution to (27) with $M = L_2(\bar{\alpha})$.

5.4. The interval width, M

To get a more direct link between the solution w and M we consider how $\bar{\alpha}(p)$, $\bar{\beta}(p)$ and $L_1(\bar{\alpha}(p))$ depend on p. A calculation shows that $\bar{\alpha}(p)$ and $\bar{\beta}(p)$ are increasing functions of p while $L_1(\bar{\alpha}(p))$ is a decreasing function of p. Hence, increasing M increases $w(-\pi/2)$ and $w(0)$.

A solution w of (27) will be stable if its maximum value is less than w_2. This maximum is equal to $w(0)$ and is an increasing function of M. A numerically computed graph of $w(0)$ against M is shown in figure 7(*a*).

The critical interval width M_c is the value of M for which $w(0) = w_2$. For applications to the full system it is important to see how M_c depends on R. Intuitively M_c will be a decreasing function of R since increasing R will raise the temperature of the black phase. To prove that $M_c'(R) < 0$ for $w_1 < w < w_2$, fix M and let w be a solution of (27). Writing $y(x) = \partial w(x)/\partial R$, a calculation shows that y satisfies an equation of the form

$$y''(x) = A(x)y - B(x), \qquad y'\left(-\frac{\pi}{2}\right) = y'(0) = 0, \tag{35}$$

where $A(x)$ and $B(x)$ are positive. It follows from (35) that $y(0) > 0$. Hence, if $w(x, R_1)$ and $w(x, R_2)$ are solutions of (27) with $R_1 > R_2$ and M fixed, then $w(0, R_1) > w(0, R_2)$. The result follows. A numerically computed graph of M_c against R is shown in figure 7(*b*).

5.5. Timescale of subdivision

When $M > M_c$, the numerical results shown in figure 5 indicate the long timescales involved in the evolution of the white phase. This can be explained by using the results of section 3 and in particular equation (14). The solution $u(x, t)$, $v(x, t)$ initially approaches the unstable manifold $\mathcal{U}$ of the coexistence phase ($t = 25$ in figure 5). At this time, $v(x, t)$ is close but not equal to $\bar{v}(w)$, $u(x, t)$ is small but non-zero, while $w(x, t) < w_2$. From equation (14), $u(x, t)$, $v(x, t)$ converges to the black phase equilibrium $(0, \bar{v}(w))$ in $\mathrm{O}(\delta^{-1})$ time ($t = 500$ in figure 5). At this time, we have that $w(x, t)$ is marginally greater than w_2 and the equilibrium $(0, \bar{v}(w))$ becomes unstable. The manifold $\mathcal{U}$ now connects this equilibrium to $(\bar{u}(w), 0)$ and by equation (14) the solution takes $\mathrm{O}(\delta^{-1})$ time to reach this point ($t = 1000$ in figure 5). This approach could be formalized by exploiting the small parameter δ and using centre manifold theory [15].

Remark 2. As a sample calculation we compute $L_1'(\alpha)$ and show that it is negative. Since the integrand for $L_1(\alpha)$ has a singularity at $w = \alpha$ some care is needed. The standard trick is to use the substitution $w = \alpha u$. A routine calculation then shows that

$$2\alpha^2 L_1'(\alpha) = -2p[2(K_1(\alpha) - K_1(p))]^{-1/2} + \alpha \int_\alpha^p H(w)[2(K_1(\alpha) - K_1(w))]^{-3/2}\, \mathrm{d}w,$$

where

$$H(w) = 2[K_1(\alpha) - K_1(w)] + wK_1'(w) - \alpha K_1'(\alpha).$$

Since $H(\alpha) = 0$ and $H'(w) = wK_1'' - K_1' = -3\sigma w^4 < 0$, it follows that $L_1'(\alpha)$ is negative.

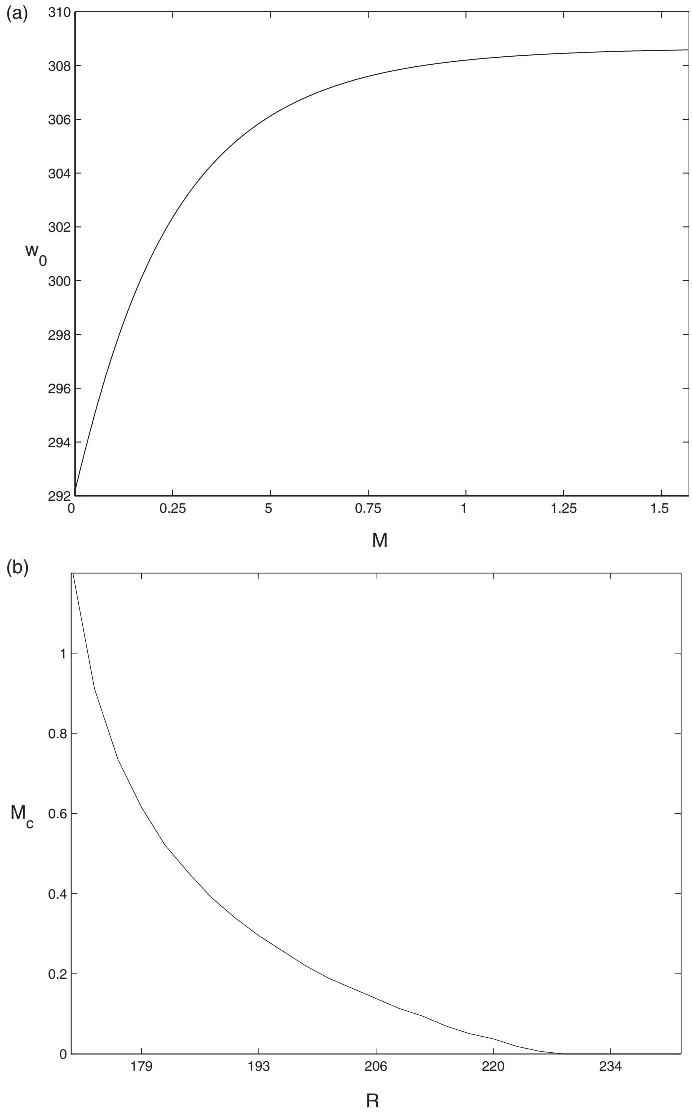

Figure 7. (*a*) Numerically determined maximum temperature, $w(0)$, depending on the width M of the black phase. Here, $R = 206.3$. Clearly $w(0)$ is an increasing function of M. (*b*) Numerically determined maximum width M_c of the single black phase depending on the solar luminosity R. Clearly, M_c is a decreasing function of R.

6. Multi-phase equilibrium solutions

Having studied the basic mechanisms of pattern formation we now briefly conjecture as to the existence, stability and convergence of more complicated patterns consisting of many white and black phase and show how the stability of such a pattern can be determined if it is periodic. We partition $I = [-\pi/2, \pi/2]$ into n intervals I_r then look for equilibrium solutions with (u, v) equal to the white phase equilibrium and black phase equilibrium on adjacent intervals. We code this by $u(x) = 0$, $v(x) = \bar{v}(w(x))$ for $x \in I_r$ with r even and $u(x) = \bar{u}(w(x))$, $v(x) = 0$

for $x \in I_r$ with r odd. Let

$$k_2(w) = [2 + \bar{v}(w)]R - \sigma w^4, \qquad k_3(w) = [2 - \bar{u}(w)]R - \sigma w^4. \tag{36}$$

Equilibrium solutions are then solutions of

$$w''(x) + k(w) = 0, \qquad w'\left(-\frac{\pi}{2}\right) = w'\left(\frac{\pi}{2}\right) = 0 \tag{37}$$

with w, w' continuous. Here, $k(w) = k_2(w)$ for $x \in I_r$ with r even and $k(w) = k_3(w)$ for $x \in I_r$ with r odd.

We conjecture that for a wide range of parameters, for a given set of intervals I_r, a solution exists. If a solution w of (37) exists such that $(w - C - 5\gamma)^2$ is not too large then it is unique (in the class of solutions enjoying the same bound). To see this, let y be the difference of two such solutions. Using (5) and (8), y satisfies the boundary value problem

$$y''(x) + A(x)y = 0, \qquad y'\left(-\frac{\pi}{2}\right) = y'\left(\frac{\pi}{2}\right) = 0, \tag{38}$$

where $A(x) < 0$. Multiplying the above equation by y and integrating proves that y is zero.

6.1. Stability

For the single phase problem considered in the previous section, the condition for stability was that the black phase interval length had to be less than some number. For (37), a solution will be stable only if $w_1 < w(x) < w_2$ for all x. If w is stable then none of the black phase intervals I_r can be too long since otherwise $w(x) > w_2$ for some x. Similarly, there will be a bound on the lengths of the white phase intervals. If all of the lengths of the black phase intervals are small, then we conjecture that w will be unstable if $\bar{w}_u < w_1$ since a solution of (37) would need w to be close to $\bar{w}_u$. It would be interesting to find out which sets of intervals I_r produce a stable equilibrium.

6.2. Convergence

Numerical solutions of equations (1)–(3) suggest convergence to an equilibrium solution of (37). Suppose $\bar{w}(x)$ is a solution of (37) with $w_1 < \bar{w}(x) < w_2$. We have not proved that $(\bar{u}(\bar{w}(x)), \bar{v}(\bar{w}(x)), \bar{w}(x))$ is a stable equilibrium solution of equations (1)–(3). For a heuristic argument to support the observed numerical solutions, suppose $w(x, t)$ is a solution of (3) with $w_1 < w(x, t) < w_2$. Then, we would expect that there would be intervals I_r such that $(u(x, t), v(x, t))$ would converge to $(0, \bar{v}(w))$ for $x \in I_r$ if r is even and to the white phase if r is odd. Replacing u and v in (3) by either $(0, \bar{v}(w))$ or $(\bar{u}(w), 0)$ we obtain a single equation for w:

$$\frac{\partial w}{\partial t} = \phi(w) + \frac{\partial^2 w}{\partial x^2} \tag{39}$$

with $\phi(w) = [2 + \bar{v}(w)]R - \sigma w^4$ for $x \in I_r$ and r even and $\phi(w) = [2 - \bar{u}(w)]R - \sigma w^4$ for $x \in I_r$ and r odd. Equation (39) has the Lyapunov function

$$E(w) = \int_{-\pi/2}^{\pi/2} \left[\frac{w_x^2}{2} - \Phi(w)\right] \mathrm{d}x, \tag{40}$$

where $\Phi' = \phi$. We obtain by differentiation and an integration by parts

$$\frac{\mathrm{d}E(w)}{\mathrm{d}t} = -\int_{-\pi/2}^{\pi/2} w_t^2 \, \mathrm{d}x. \tag{41}$$

This implies [14] that such a solution would converge to the set of solutions of equation (37).

6.3. Periodic patterns

If the intervals I_r are periodically arranged then we can construct a solution of (37). Fix x_1 and x_2 and let w be a solution on $[0, x_1 + x_2]$ of

$$\begin{aligned} w''(x) + k_3(w) &= 0 \qquad \text{for } 0 < x < x_1, \\ w''(x) + k_2(w) &= 0 \qquad \text{for } x_1 < x < x_1 + x_2 \end{aligned} \tag{42}$$

with $w'(0) = w'(x_1 + x_2) = 0$ and w, w' continuous. Solutions of (42) can be studied in the same way as the single phase problem in the previous section. If we extend the solution w of (42) as an even function of period $2(x_1+x_2)$ then w will be a solution of (37) if $(x_1+x_2)n = \pi/2$ for some integer n. The minimum of w is $w(0)$ and the maximum is $w(x_1+x_2)$ and we would expect w to be stable if $w_1 < w(0)$ and $w(x_1 + x_2) < w_2$.

7. Discussion

In this paper, we have studied a spatial version of daisyworld based on a one-dimensional projection of a plane. Numerical results show that this system of two static populations which affect a third diffusing 'reagent' (temperature) generates striped patterns when subjected to spatially non-uniform perturbations. Analysing the system formally shows that the stability of the coexistence equilibrium is the key to this behaviour due to a small eigenvalue, the sign of which is easily switched. If the temperature (w) is fixed then this eigenvalue is positive and coexistence is unstable. If heat is allowed to diffuse the eigenvalue becomes negative and coexistence is stable. However, a non-constant perturbation causes it to switch again, rendering the solution unstable. Consideration of a related problem, in which a single stripe is permitted, reveals a second instability mechanism which determines a maximum stripe width. This leads to additional patterning by forcing stripes exceeding the maximum width to subdivide. Analysis of multiphase patterns is not straight forward. Temperature profiles are constructed for periodic patterns but, in general, this is a non-trivial, global problem.

There are two possible extensions to this model which we consider briefly. First, the inclusion of a term to represent daisy diffusion may be expected to smooth the striped pattern of the solution. However, numerical solutions of equations (1)–(3) with the term $\epsilon(u_{xx} + v_{xx})$ for ϵ of order 10^{-2} added to the right-hand side of equations (1) and (2) show that the striped patterns persist. Second, equations (1)–(3) are a simplified form of equations (A11)–(A13) which are a one-dimensional projection of a spherical model. Numerical solutions of equations (A11)–(A13) display similar characteristics to those discussed (figure 8) and it is reasonable to assume that similar mechanisms are operating. The most significant differences arise from the cosine distribution for $\bar{R}(x)$. As a result of this, temperature conditions for coexistence ($w_1 < w < w_2$) only occur over part of the region, the extent of which depends on R. However, regardless of external perturbations, the numerical results indicate that 'competitive exclusion' and stripe formation always occurs.

Although this paper has been primarily concerned with the mathematics of the system, further numerical experiments [13] have shown that the one-dimensional daisyworld retains similar properties to the zero-dimensional model [1]. Under a gradual increase in $\bar{R}(x)$ the striped pattern frequently adjusts in order to maintain a stable pattern but this does not compromise the regulation of global temperature. Daisyworld is intended to be a tutorial model and so there is no direct comparison with the real world. However, both the model and the true vegetation of the Earth appear to have the potential for multiple stable states dependent on initial conditions. In the model these correspond to the different patterns of black and white colonies. In the real world there are a number of regions in which two

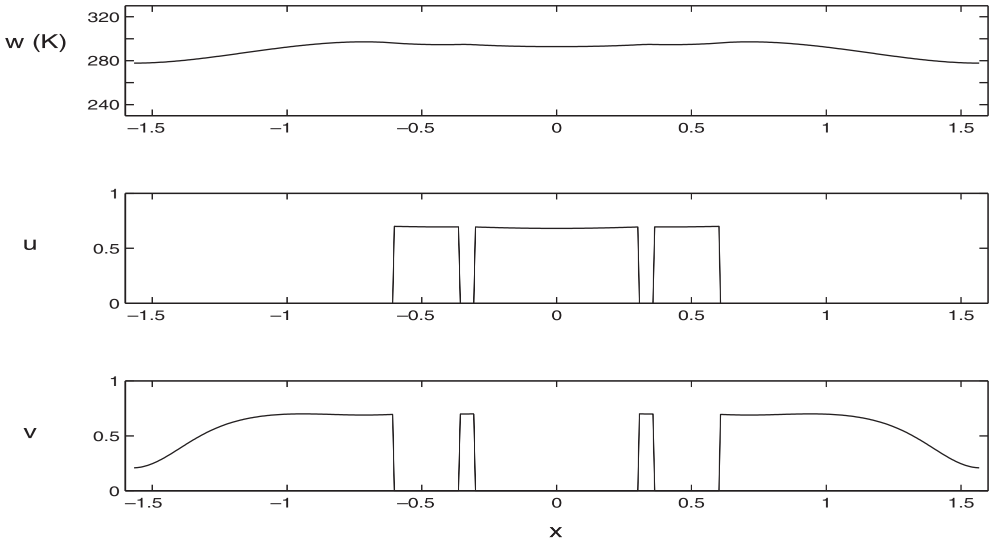

Figure 8. Numerical solution at $t = 1000$ (taken to be equilibrium) of the spherical-based one-dimensional daisyworld given by equations (A11)–(A13) with $\bar{R}(x) = 206.3\cos(x)$. Initially $u(x) = v(x) = 0.001$, $w(x) = 292$ for all x. The striped patterning is similar to that observed in the model derived from a plane, but no perturbation is required to initiate them.

alternative ecosystems could exist by modifying the local climate. For instance it is believed that, under the same global climate, the Sahara region could be covered by dense vegetation instead of desert [17], the Amazon rain forest could be arid pasture [18] and the Great Plains of North America could be extensively wooded [19]. Perhaps the most intriguing point arising from the daisyworld model is that not all patterns are stable. If a pattern which does not regulate both the local and global climate is introduced then it will quickly adjust to one which does. In the real world the interactions between the vegetation and climate are no doubt different and significantly more complex. However, the results from daisyworld suggest that one factor influencing the distribution of vegetation over the real Earth's surface may be the requirement for a pattern capable of global climate regulation. It is possible that there are a finite number of such distributions and these determine the possible stable states of the system.

Acknowledgments

The authors thank Andrew White, Jonathan Sherratt and Tim Lenton for helpful discussion. BA is supported by an EPSRC studentship.

Appendix. Description of the model and its relationship to the zero-dimensional form

For completeness, the equations for the original daisyworld model [1] and their extension to one dimension [13] are described briefly here.

The surface temperature w of the planet is found by assuming that at equilibrium, the black body radiation equals the solar energy absorbed at the surface. Thus, w is the equilibrium solution of:

$$\frac{\mathrm{d}w}{\mathrm{d}t} = (1 - A)R^* - \sigma w^4, \tag{A1}$$

where R^* is the energy reaching the surface from the sun, A is the surface albedo and σ is the Stefan–Boltzmann constant. The surface albedo is given by

$$A = A_g\alpha_g + A_w u + A_b v, \tag{A2}$$

where A_g, A_w and A_b are the albedoes of bare ground, white daisies and black daisies, respectively, and α_g, u and v are the corresponding areas as a proportion of 1. The local temperatures of each daisy type are given by

$$T_w = q(A - A_w) + w \qquad \text{and} \qquad T_b = q(A - A_b) + w. \tag{A3}$$

Here, q is a implicit measure of heat diffusion between the three surfaces in the longitudinal direction. This is assumed to operate very locally and is independent of the regional-scale diffusion represented by the Laplacian operator.

Two ordinary differential equations, based on an area competition model [16] describe the dynamics of the daisies:

$$\frac{\mathrm{d}u}{\mathrm{d}t} = u(\alpha_g\beta_w - \gamma) \qquad \text{and} \qquad \frac{\mathrm{d}v}{\mathrm{d}t} = v(\alpha_g\beta_b - \gamma), \tag{A4}$$

where γ is the (constant) death rate and β_w, β_b are parabolic growth rates given by:

$$\beta_w = 1 - \delta(C - T_w)^2 \qquad \text{and} \qquad \beta_b = 1 - \delta(C - T_b)^2. \tag{A5}$$

Here δ is a small constant and C is the optimum temperature for growth.

Setting $A_g = 0.5$, $A_w = 0.25$, $A_b = 0.75$ and $q = 20$ (the parameter values used in the original model [1]), equation (A2) becomes:

$$A = \frac{1-u-v}{2} + \frac{u}{4} + \frac{3v}{4} = \frac{2-u+v}{4} \tag{A6}$$

and the equations in (A3) become:

$$T_w = 5(u - v - 1) + w \qquad \text{and} \qquad T_b = 5(u - v + 1) + w. \tag{A7}$$

Using this leads to the ordinary differential equation model:

$$\frac{\mathrm{d}u}{\mathrm{d}t} = u[(1 - \delta[C - 5(u - v - 1) + w]^2)(1 - u - v) - \gamma], \tag{A8}$$

$$\frac{\mathrm{d}v}{\mathrm{d}t} = v[(1 - \delta[C - 5(u - v + 1) + w]^2)(1 - u - v) - \gamma], \tag{A9}$$

$$\frac{\mathrm{d}w}{\mathrm{d}t} = (2 - u + v)R - \sigma^4 w \tag{A10}$$

with $R = R^*/4$.

Finally, a term to represent heat diffusion is added to the right-hand side of equation (A10). For the simplified model in the plane this is the one-dimensional Cartesian Laplacian, giving equation (3). For the model operating on the surface of a sphere this is the spherical Laplacian (with r and ϕ constant since only one dimension is considered). For the spherical case we must also take into account the uneven distribution of solar radiation over the surface. Thus, R is weighted using a cosine function: $\bar{R}(x) = R\cos(x)$. The three equations describing the one-dimensional projections of the spherical system are then:

$$\frac{\partial u}{\partial t} = u[(1 - \delta[C - 5(u - v - 1) - w]^2)(1 - u - v) - \gamma], \tag{A11}$$

$$\frac{\partial v}{\partial t} = v[(1 - \delta[C - 5(u - v + 1) - w]^2)(1 - u - v) - \gamma], \tag{A12}$$

$$\frac{\partial w}{\partial t} = (2 - u + v)\bar{R}(x) - \sigma w^4 + \frac{1}{\cos(x)}\frac{\partial}{\partial x}\left(\cos(x)\frac{\partial w}{\partial x}\right). \tag{A13}$$

References

[1] Watson A J and Lovelock J E 1983 Biological homeostasis of the global environment: the parable of daisyworld *Tellus* B **35** 284–9

[2] Lovelock J E 1988 *The Ages of Gaia. A Biography of Our Living Earth* (Oxford: OUP)

[3] Margulis L and Lovelock J E 1974 Biological modulation of the Earth's atmosphere *Icarus* **21** 471–89

[4] De Gregorio S, Pielke A and Dalu G A 1992 Feedback between a simple biosystem and the temperature of the Earth *J. Nonlinear Sci.* **2** 263–92

[5] Saunders P T 1994 Evolution without natural selection: further implications of the daisyworld parable *J. Theor. Biol.* **166** 365–73

[6] Weber S L 2001 On homeostasis in daisyworld *Climatic Change* **48** 465–85

[7] Harding S P and Lovelock J E 1996 Exploiter-mediated coexistence and frequency-dependent selection in a numerical model of biodiversity *J. Theor. Biol.* **182** 109–16

[8] Robertson D and Robinson J 1998 Darwinian daisyworld *J. Theor. Biol.* **195** 129–34

[9] Lenton T M and Lovelock J E 2000 Daisyworld is Darwinian: constraints on adaptation are important for planetary self-regulation *J. Theor. Biol.* **206** 109–14

[10] von Bloh W, Block A and Schellnluder H J 1997 Self-stabilization of the biosphere under global change: a tutorial geophysical approach *Tellus* B **49** 249–62

[11] Koeslag J H, Saunders P T and Wessels J A 1997 Glucose homeostasis with infinite gain: further lessons from the daisyworld parable? *J. Endocrinol.* **154** 187–92

[12] Brown P N, Byrne G D and Hindmarsh A C 1989 VODE: a variable coefficient ODE solver *SIAM J. Sci. Stat. Comput.* **10** 1038–51

[13] Adams B, Carr J, Lenton T M and White A 2003 One-dimensional daisyworld: spatial interactions and pattern formation *J. Theor. Biol.* at press

[14] Henry D 1981 *Geometric Theory of Semilinear Parabolic Equations (Lecture Notes in Mathematics vol 840)* section 4.3 (Berlin: Springer)

[15] Carr J 1981 *Applications of Centre Manifold Theory (Applied Math. Sciences vol 35)* section 2.7 (Berlin: Springer)

[16] Carter R N and Prince S D 1988 Epidemic models used to explain biogeographical distribution limits *Nature* **293** 644–5

[17] Brovkin V, Claussen M, Petoukhov V and Ganopolski A 1998 On the stability of the Sahara/Sahel region *J. Geophys. Res.* **103** 31613–24

[18] Shukla J, Nobre C and Sellers P 1990 Amazon deforestation and climate change *Science* **247** 1322–5

[19] Woodcock D W 1992 The rain on the plain: are there vegetation-climate feedbacks? *Global Planet. Change* **97** 191–201